CVD Synthesis and Gas Permeation Properties of Thin Palladium/Alumina Membranes

George Xomeritakis and Yue-Sheng Lin
Dept. of Chemical Engineering, University of Cincinnati, Cincinnati, OH 45221

Thin (0.5–5-μm) palladium (Pd) membranes were prepared inside pores or on the surface of mesoporous (pore size 4–6 nm), sol–gel-derived γ-Al_2O_3 supports by the chemical vapor deposition (CVD) method using palladium acetylacetonate and palladium chloride (together with hydrogen) as Pd precursors. When Pd is deposited in the form of metal plugs inside pores of γ-Al_2O_3, He permeance of the composite membranes increases exponentially with temperature, indicating activated diffusion through the microporous metal deposit defects, while only modest permselectivity for H_2 is observed. When Pd is deposited in the form of a metal film on the surface of γ-Al_2O_3, He permeance is governed by Knudsen-viscous flow through meso/macroporous metal film defects. The H_2 permeance of different palladium membranes prepared by CVD appears to increase with palladium crystal grain size. The highest H_2 permeance and H_2:He permselectivity for membranes prepared in this study are about $1.0-2.0\times10^{-7}$ $mol\cdot m^{-2}\cdot s^{-1}\cdot Pa^{-1}$ and 200–300 at 300°C, respectively.

Introduction

Palladium and its alloys, especially in the form of thin films, have potential for applications as membranes for chemical reaction or gas separation involving hydrogen. Table 1 gives H_2 permeance data of common inorganic materials that can be used for H_2 separation at elevated temperatures. As can be seen from this table, Pd-based membranes offer higher H_2 permeation rates at much lower temperature compared to SiO_2 and appear to be more attractive for application in large-scale gas-separation processes. Since porous inorganic supports are readily available, preparation of supported thin palladium membranes by liquid- or vapor-phase deposition processes has recently been a subject of extensive research (Hsieh, 1996). Such supported palladium membranes are believed to offer higher H_2 permeation flux, better mechanical strength, and reduced material costs as compared with the traditional symmetric palladium membranes.

The preparation of supported Pd membranes on macroporous ceramic, glass, or metal supports has been recently addressed by the electroless plating technique (Uemiya et al., 1991a,b; Govind and Atnoor, 1991; Collins and Way, 1993; Yeung and Varma, 1995; Jemaa et al., 1996). This technique offers advantages such as simple and low-cost equipment for membrane preparation as well as easiness in coating large surface area and complex-shaped supports, which is essential to metallic membrane commercialization. On the other hand, electroless plating is a rather cumbersom and time-consuming process, requiring a number of pretreatment (activation and sensitization) steps before final plating of the desired metal is achieved. Because of the use of macroporous inorganic supports and the poor control over the metal-film thickness offered by the method, electroless-plated palladium membranes are usually rather thick (>5 μm) and have poor mechanical stability against temperature or hydrogen pressure cycles, known also as embrittlement.

Lin and coworkers (Jayaraman et al., 1995; Jayaraman and Lin, 1995) reported the first attempt to prepare ultrathin (<0.5 μm) Pd and Pd/Ag alloy membranes on mesoporous ceramic supports by radio-frequency (rf) magnetron sputtering technique. They also conducted an extensive investigation on the effect of the various synthesis conditions and support characteristics on the gas transport properties of the metallic membranes. Bryden and Ying (1995) reported a similar effort employing direct current (DC) magnetron sputtering to deposit nanostructured Pd films on mesoporous glass supports.

Correspondence concerning this article should be addressed to Y.-S. Lin.

Table 1. Transport Properties of H_2-Semipermeable Membranes

Membrane Material	Thickness (μm)	Temp. (°C)	H_2 Flux* (std. cm^3/cm^2)	Selectivity (H_2/N_2)	Reference
γ-Al_2O_3**	5.0	25	94.0	3.7	Lin and Burggraaf (1991a)
Dense silica	0.1	700	8.5	7500	Kim and Gavalas (1995)
Palladium	4.5	400	25.4	∞	Uemiya et al. (1991a)
Pd/Ag alloy	5.8	400	36.8	∞	Uemiya et al. (1991b)

*H_2 partial pressure 2 atm at feed side; 1 atm at permeate side.
**Pore size 4 nm.

Ceramic-supported, submicron-thick Pd-based metallic membranes with substantial permselectivity for H_2 at elevated temperatures were synthesized only recently by Xomeritakis and Lin (1997), employing dc magnetron sputtering. Despite this preliminary success, however, these membranes, just as with those prepared by the electroless plating method, are still weak against embrittlement induced by temperature or hydrogen pressure cycles.

Deposition of Pd *inside* pores of ceramic supports may overcome the problems associated with the mechanical stability of Pd membranes. Furthermore, palladium-plugged ionic-conducting ceramic composites may have potential for use as the electrolytes for solid oxide fuel cells or membranes for oxygen separation (Mazanec, 1996). Morooka and coworkers (Yan et al., 1994; Morooka et al., 1995) first demonstrated the feasibility of preparing a dense, 2–5-μm-thick Pd membrane inside macropores of α-Al_2O_3 tubes by low-pressure metallorganic CVD (MOCVD) employing a commercially available metallorganic palladium precursor (Pd acetate). Their membrane exhibited high H_2 permeation flux and H_2:N_2 permselectivity and good stability against temperature cycling in a H_2 atmosphere. Uemiya and coworkers (Uemiya et al., 1994, 1996) also reported successful preparation of a Pd membrane inside pores of α-Al_2O_3 tubes by atmospheric pressure MOCVD employing Pd acetylacetonate as metal source. The success of those workers indicates that reactive vapor deposition is an attractive approach for confining Pd inside porous supports for the purpose of preparing dense supported H_2-permselective membranes with improved properties. Nevertheless, efficient plugging of support macropores with Pd still remains a difficult task and may hamper commercialization of such metallic/ceramic membrane composites.

Xomeritakis and Lin (1996) recently reported successful deposition of Pd inside pores of mesoporous alumina supports (pore size < 10 nm) using a counterdiffusion CVD scheme with H_2 and $PdCl_2$ as metal precursors. Despite the difficulties associated with the use of the chloride as Pd source, proper experimental conditions were identified that resulted in submicron-thick and fairly dense Pd membranes. The main objectives of this study are to demonstrate controlled deposition of palladium inside pores or on the surface of mesoporous alumina supports by a more efficient MOCVD process and to study the gas transport properties of such nanostructured palladium–alumina membrane composites. A comparison is also made with the corresponding properties of Pd membranes made from the chloride precursor. An attempt to correlate the gas transport properties of the palladium–ceramic composites to their microstructure is presented.

Experimental

Palladium membrane preparation

Figure 1 is a SEM image of the cross section of a two-layer support used for Pd membrane preparation, showing a 10-μm-thick, mesoporous γ-Al_2O_3 layer coated on the surface of a macroporous α-Al_2O_3 disk by the sol–gel process. The α-Al_2O_3 disks were prepared by pressing α-Al_2O_3 powder (Phillips) in a stainless-steel mold followed by calcination at 1150°C for 30 h. One surface of the disks was polished with SiC papers of different roughness and then γ-Al_2O_3 was coated by dipping the disks in a 1-M boehmite sol doped with polyvinyl alcohol (PVA) followed by drying and calcination at 450°C for 3 h (Chang et al., 1994). The properties of the two-layer ceramic supports are summarized in Table 2. Figure 2 shows the hot-wall CVD reactor used in this study. The reactor is divided into two chambers by the support with the γ-Al_2O_3 layer facing the metal precursor sublimation boat, while hydrogen can be separately introduced into the opposite chamber.

MOCVD experiments employing Pd acetylacetonate as the palladium source were carried out in two different modes or reaction schemes. Table 3 summarizes the conditions used. In mode I, N_2 carrier was fed over the sublimation boat to carry precursor vapor toward the γ-Al_2O_3 top layer, while the opposite reactor chamber was continuously evacuated with no feed of N_2 or H_2. This experimental condition was chosen in order to favor infiltration and subsequent decomposition of precursor vapors *inside* the support pores. In mode II, N_2 was fed in both chambers at the beginning of the experiment while H_2 was introduced in the second chamber when the substrate temperature was 100–150°C lower than

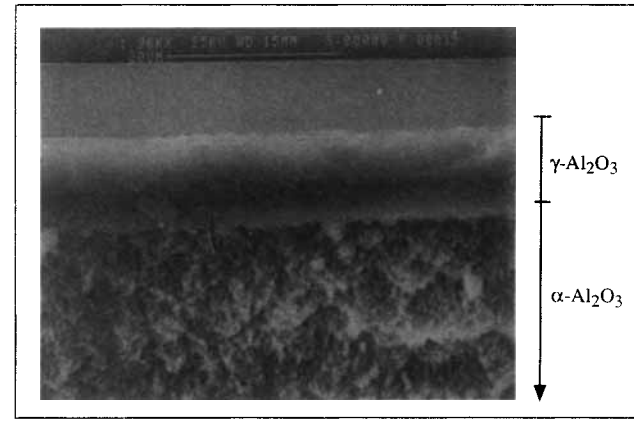

Figure 1. SEM image of the cross section of a two-layer alumina support used for CVD of Pd.

Table 2. Properties of Two-Layer Supports Used for Pd Membrane Preparation

No.	Pore Size (nm)	Porosity (%)	Thickness (μm)
γ-Al_2O_3	4–6	40	5–10
α-Al_2O_3	200–220	50	2000

the final setpoint. This experimental condition was chosen in order to secure precursor reduction and metal growth primarily *outside* the support surface. Complementary counter-diffusion CVD (CD-CVD) experiments using palladium chloride and hydrogen in order to grow Pd primarily *inside* the support pores were performed as described previously (Xomeritakis and Lin, 1996). In all the CVD experiments described earlier, the location of Pd precursor inside the reactor was chosen so that precursor sublimation became significant when substrate temperature reached the specified setpoint.

Multicomponent permeation experiments

The permeation properties of the Pd membranes were determined in a multicomponent permeation setup consisting of a feed delivery section, a permeation temperature control section, and a permeate composition analysis section. Figure 3 shows the experimental setup. The permeation cell was custom-made to hold the composite disk-shaped membranes with the aid of silicon rubber O-rings. An equimolar mixture of H_2 and He with balance Ar was introduced over the Pd-coated surface of the substrate while N_2 was introduced over the opposite membrane side to collect the permeate. Composition analysis was performed with a HP 5890 Series II gas chromatograph unit equipped with a molecular sieve 13 X packed column and a thermal conductivity detector operated with N_2 carrier. The membrane permeance for component (i) was calculated using the equation:

$$F_i = \frac{y_i Q_s}{(x_i - y_i) P_o S_m}, \qquad (1)$$

where Q_s is the sweep gas flow rate (mol·s^{-1}); S_m is the membrane permeation area (m^2); x_i is the mole fraction of component (i) in the feed; y_i is the mole fraction of component (i) in the sweep, determined by the GC; P_o is the total pressure of both feed and sweep gas streams (= 1 atm); F_i is the membrane permeance of component (i) (mol·m^{-2}·s^{-1}·Pa^{-1}).

Table 3. Experimental Conditions for MOCVD of Pd

Parameter	Mode I	Mode II
Deposition temperature	200–500°C	300–350°C
Sublimation boat temperature	100–150°C	100–150°C
N_2 flow rate toward γ-Al_2O_3 layer	5 mL(STP)/min	5 mL(STP)/min
N_2 flow rate toward α-Al_2O_3 support	—	4 mL(STP)/min
H_2 flow rate toward α-Al_2O_3 support	—	1 mL(STP)/min
Reactor pressure	1 mbar	1 mbar
Deposition time	1–4 h	1 h

Membrane characterization

The presence of palladium inside pores or on the surface of the γ-Al_2O_3 support and its extent of crystallinity were analyzed by an X-ray diffractometer (Siemens, CuK_α). In addition, the morphology, thickness, and location of the Pd deposits were studied by examining the cross sections of the support disks with a field-emission scanning electron microscope (Hitachi S-4000) equipped with secondary and backscattered electron detectors and EDS analysis unit.

Results

Membrane morphology

Figure 4 shows a secondary electron (SE) image and Pd and Al X-ray line mapping of the cross section of a membrane made by MOCVD under conditions of mode I. From the SE image, no distinct metal film is observed outside the top layer. However, the intensity distribution in the X-ray mapping images indicates that Pd is present inside the γ-Al_2O_3 layer with a maximum intensity near the γ-Al_2O_3 surface that drops exponentially along its thickness to a zero value near the γ-Al_2O_3/α-Al_2O_3 interface. This Pd profile

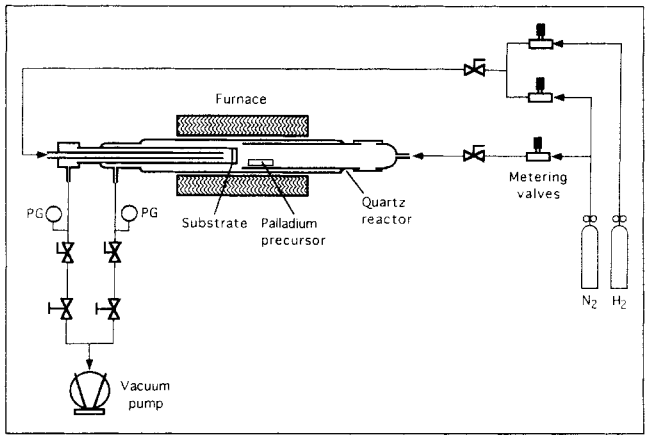

Figure 2. Experimental setup for CVD of Pd.

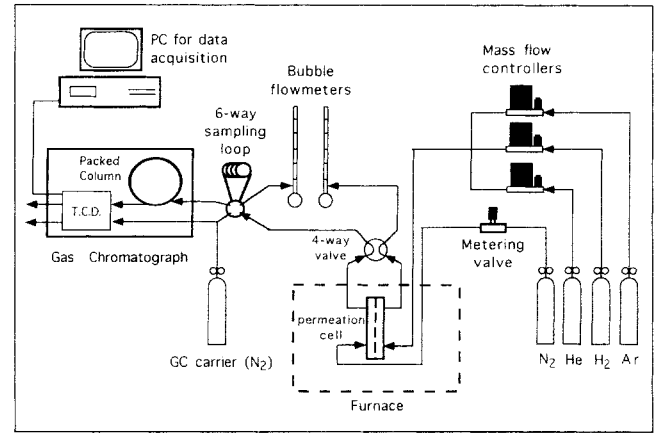

Figure 3. Multicomponent gas permeation setup.

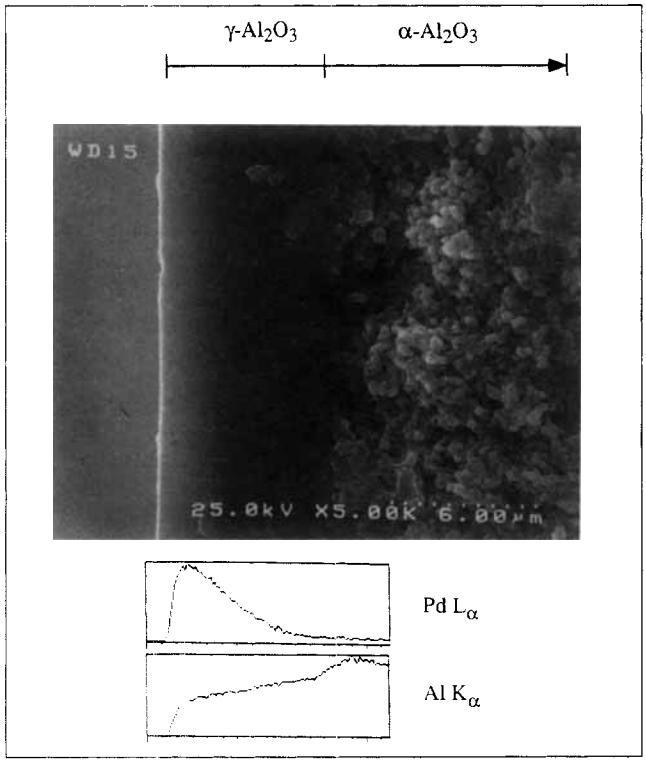

Figure 4. Secondary electron image and X-ray line mapping of Pd and Al, of the cross section of a two-layer support after deposition of Pd by MOCVD under conditions of mode I (type A membrane).

determined by SEM/EDS within the γ-Al_2O_3 layer is consistent with predictions of a mathematical model describing MOCVD inside porous substrates accounting for simultaneous diffusion and decomposition reaction of vapor precursor inside substrate pores (Xomeritakis et al., 1996). Figure 5

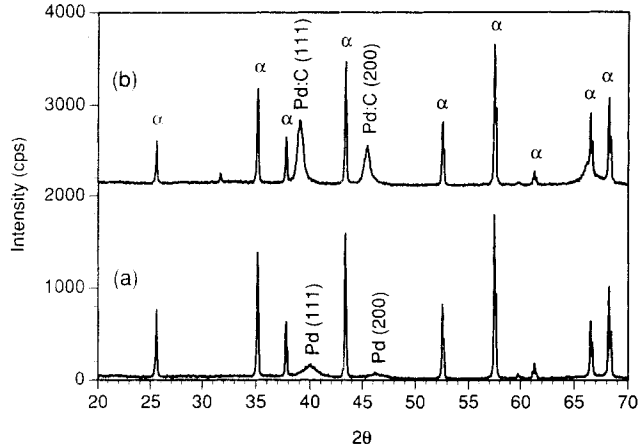

Figure 5. XRD patterns of Pd membranes made by MOCVD under conditions of mode I (type A membrane).

(a) After permeation at 350°C; (b) after further *in-situ* heat treatment at 700°C for 3 h. Peaks indexed with "α" are assigned to the α-Al_2O_3 substrate.

shows XRD patterns of two different membrane samples prepared by MOCVD under conditions of mode I with the substrate held at 350°C during deposition. Sample (b) was further subjected to *in-situ* heat treatment at 700°C for 3 h. As seen from Figure 5a, Pd is poorly crystallized in the standard fcc structure after deposition at 350°C, with grain size usually < 5 nm. After heat treatment, peak resembling those of fcc Pd, but with larger lattice parameter (3.99 Å, as determined from the (111) and (200) d-spacings) than pure (3.89 Å), start to appear, with the grain size about 15 nm larger than those of membranes not subjected to heat treatment. These results suggest that a significant amount of unreacted precursor or organic ligand is trapped inside the support pores during MOCVD under conditions of mode I, which is further transformed to carbon incorporated in the Pd lattice during heat treatment at higher temperatures.

Maruyama and Shirai (1995) found that growth of Cu films on dense glass substrates from Cu(II) acetylacetonate could only be achieved above 220°C in the presence of H_2, while no metal growth was observed in an inert atmosphere (N_2). This evidence indicates that the rate of metal-forming reaction strongly depends on temperature and H_2 content in the deposition environment. In the case of a porous substrate, it is likely that a slow reaction favors precursor penetration inside the substrate pores resulting in broad deposits, which is consistent with the predictions of theoretical models taking into account the effect of reaction and diffusion competition on the CVD deposit morphology (Lin and Burggraaf, 1991b; Xomeritakis and Lin, 1994). On the other hand, CD-CVD from the chloride precursor in the presence of hydrogen resulted in thinner Pd deposits (≈ 1.4 μm) as observed from the backscattered electron image shown in Figure 6, a result

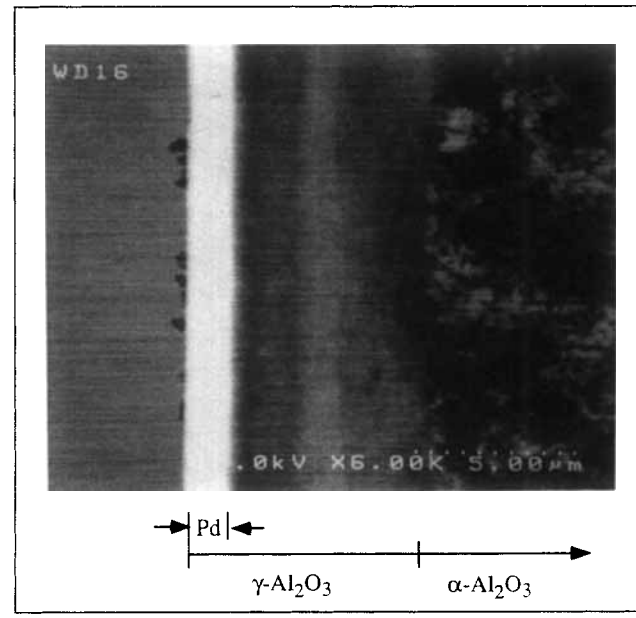

Figure 6. Backscattered electron image of the cross section of a two-layer support after deposition of Pd by CD-CVD from the chloride precursor (type C membrane), showing a 1.4-μm-thick Pd zone inside the γ-Al_2O_3 layer very close to its surface.

of faster consumption of metal precursor vapor inside support pores in the presence of hydrogen.

In addition, even if reaction proceeds to completion, the ligand molecules will have less chance to diffuse out of the small pores of γ-Al_2O_3, resulting in trapping of organic material and contamination of metal grown inside pores. Attempts to improve the yield of Pd deposition by increasing the substrate temperature were quite unsuccessful since carbon formation by pyrolytic decomposition of the ligand molecules became increasingly important at the same time. Yan et al. (1994) claimed success in growing metallic Pd with large grain size (about 80 nm) *inside* pores of α-Al_2O_3 tubes by thermal decomposition of Pd(II) acetate vapor at 300–500°C. However, the situation was different in that study since support pore size was much larger (about 150 nm) than molecular dimensions and decomposition products could readily desorb and diffuse outside the support without interferring with the growing metal grains.

Figure 7 shows the XRD pattern of a Pd membrane made by MOCVD under conditions of mode II with substrate held at 350°C. The XRD pattern indicates the presence of pure Pd, well crystallized in the standard fcc structure (grain size 30–50 nm). The membrane surface after deposition bears a lustrous, reflective, and electrically conducting metal layer. Figure 8 reveals that this metal layer is about 0.8 μm thick and lies on the surface of the γ-Al_2O_3 top layer. In contrast, after MOCVD with conditions under mode I or CD-CVD from the chloride precursor, the membrane surface has black, indicating infiltration of metal inside the γ-Al_2O_3 pores. This remarkable difference in the deposition result of modes I and II further supports that H_2 increases dramatically the rate of Pd formation during MOCVD by facilitating the breakage of the Pd–O bonds of the metal with the acetylacetonate ligand. On the other hand, the early introduction of H_2 during MOCVD in mode II results in saturation of the γ-Al_2O_3 surface with adsorbed H_2, which readily reacts with the carried precursor, thus preventing deep penetration of the latter inside the support pores. As shown in Table 3, substrate temperature was varied within a narrow optimal range to secure appreciable metal growth rate while minimizing incorporation of impurities due to pyrolytic decomposition of organic ligand molecules.

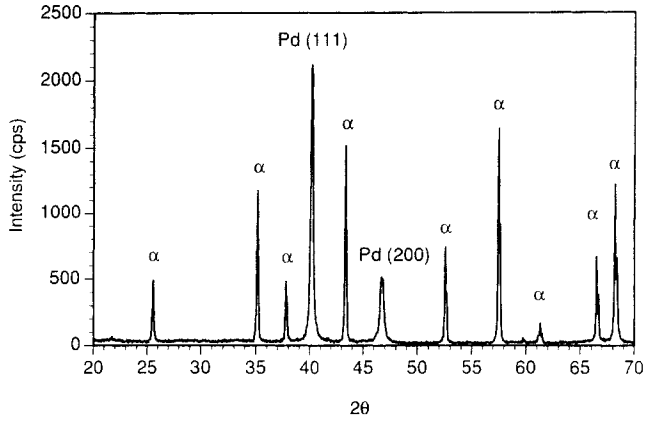

Figure 7. XRD pattern of a Pd membrane made by MOCVD under conditions of mode II (type B membrane), showing peaks of fcc Pd among α-Al_2O_3 substrate peaks.

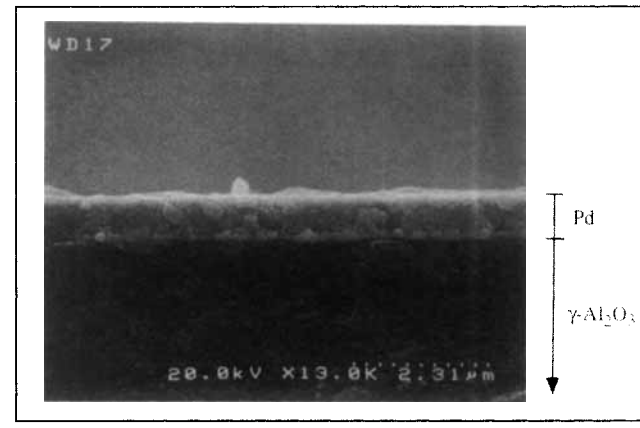

Figure 8. SEM image of the cross section of a two-layer support after deposition of Pd by MOCVD under conditions of mode II (type B membrane), showing a 0.8-μm-thick Pd film deposited on the γ-Al_2O_3 surface.

Membrane permeation properties

After preparation, the Pd membranes made by CVD were roughly checked for gas tightness by measuring the He permeance at room temperature in a single gas permeation setup described in detail elsewhere (Xomeritakis and Lin, 1996). Table 4 shows typical He permeance data of the ceramic supports and the Pd membranes made under different conditions. In the case of MOCVD under conditions of mode I, the permeance of the support decreased by three to four orders of magnitude, indicating efficient plugging of γ-Al_2O_3 pores by Pd (together with organic material). This result was better than that reported previously (Xomeritakis and Lin, 1996), since Pd membranes made by CD-CVD from the chloride precursor (type C membranes in Table 4) exhibited only about two to three orders of magnitude reduction in He permeance compared to the support. Type B membranes made by MOCVD under conditions of mode II exhibited larger He permeance compared to type A membranes, primarily because of the difficulty in growing fairly dense and thin (< 1 μm) metal films on the γ-Al_2O_3 surface. Although these metal films macroscopically appear continuous, small dust particles or surface defects are enough to create pinholes that deteriorate membrane gas tightness as evidenced from He permeation experiments.

The He permeance of the Pd membranes at elevated temperatures was determined in the setup shown in Figure 3. Figure 9 shows He permeance vs. temperature of two differ-

Table 4. He Permeance at Room Temperature (T) of Support and Pd Membranes Made by CVD

Membrane Type	Reaction Scheme	Pd Location vs. γ-Al_2O_3	He Permance ($mol \cdot m^{-2} \cdot s^{-1} \cdot Pa^{-1}$)
Two-layer support	—	—	2×10^{-6}
A	MOCVD (mode I)	Inside pores	$0.2-2 \times 10^{-9}$
B	MOCVD (mode II)	On surface	$0.5-5 \times 10^{-8}$
C	CD-CVD*	Inside pores	$0.02-1 \times 10^{-8}$

*From reaction of $PdCl_2$ and H_2, see Xomeritakis and Lin (1996).

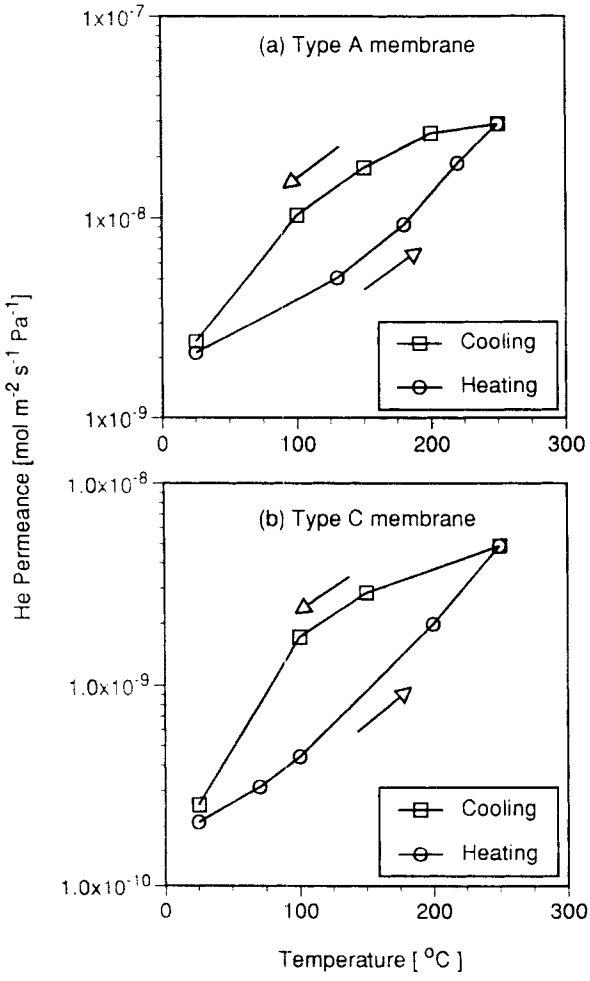

Figure 9. He permeance vs. temperature of (a) type A and (b) type C membranes measured during heating to 250°C and cooling to ambient.

ent Pd membranes prepared inside γ-Al_2O_3 pores by (a) MOCVD under conditions of mode I, and (b) CD-CVD from the chloride precursor. As seen in this figure, He permeance through these membranes (primarily through defects in the metal/ceramic structure formed by CVD inside support pores) increases 15 to 20 times after heating to 250°C and reverts back to its initial value after cooling to ambient. This effect was observed for all membrane samples prepared by depositing Pd inside γ-Al_2O_3 pores, as well as for the same membrane when the test was repeated multiple times. In the results presented in Figure 9, the He permeance values determined during heating or cooling (both at 1°C/min) do not coincide because insufficient time was allowed for thermal equilibration in the intermediate temperature points. Figure 10 shows He permeance vs. temperature of a type B membrane prepared on the surface of γ-Al_2O_3 by MOCVD under mode II conditions. The thickness of this membrane was about ≈ 1 μm as determined by SEM. As seen from this figure, He leaks through Pd defects decrease with increasing temperature when Pd is grown in the form of a metal film on the surface of the support. The relative decrease in He permeance is larger than that expected from the temperature dependence of Knudsen permeability ($\alpha\, 1/\sqrt{T}$), suggesting

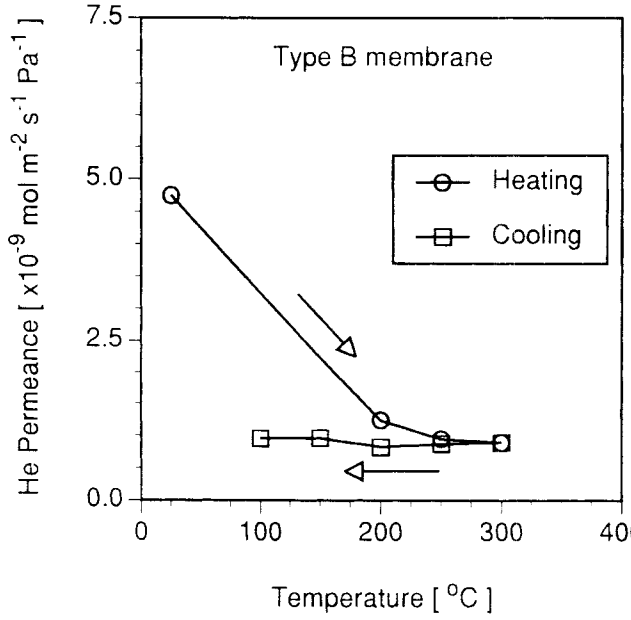

Figure 10. He permeance vs. temperature of a type B membrane measured during heating to 300°C and cooling to 100°C.

that the thin metal films undergo favorable densification during heating to high temperature.

Figure 11 shows H_2 and He permeance vs. temperature of two different Pd membranes prepared inside γ-Al_2O_3 pores by (a) MOCVD under conditions of mode I, and (b) CD-CVD from the chloride precursor. The permeance data were measured during the cooling stage of the experiment, since the membrane permeation area changed slightly due to O-ring deformation during the heating stage. For the type A membrane shown in Figure 11a, both H_2 and He permeance increase with temperature, with the H_2:He permeance ratio not exceeding the value dictated by the Knudsen mechanism (1.41). A similar trend can be seen for the type C membrane shown in Figure 11b, but with H_2:He permeance ratio well above the Knudsen value. The data shown in Figure 11 indicate that Pd membranes formed by CVD inside fine pores of γ-Al_2O_3 have very limited permselectivity for H_2 over He. Substantial permselectivity of H_2 over He was observed only for type B membranes formed on the surface of γ-Al_2O_3 by MOCVD under conditions of mode II. Figure 12 shows H_2 and He permeance data for a type B membrane grown to a thickness of 1 μm on the surface of the support. The H_2:He ratio was > 200 at 300°C, while the He leak through metal film defects was quite independent of temperature, indicating that the defects are in the mesoporous or macroporous range.

Discussion

Figure 13 shows the resistance model for gas permeation through the Pd membranes made by CVD. Prior to CVD, the resistance of gas permeation is that of the support (R_1). After CVD, helium permeates through the defects in the metal deposit (R_2) and the porous alumina support (R_1). If the Pd deposit is fairly gas tight ($R_2 \gg R_1$), the permeation rate of

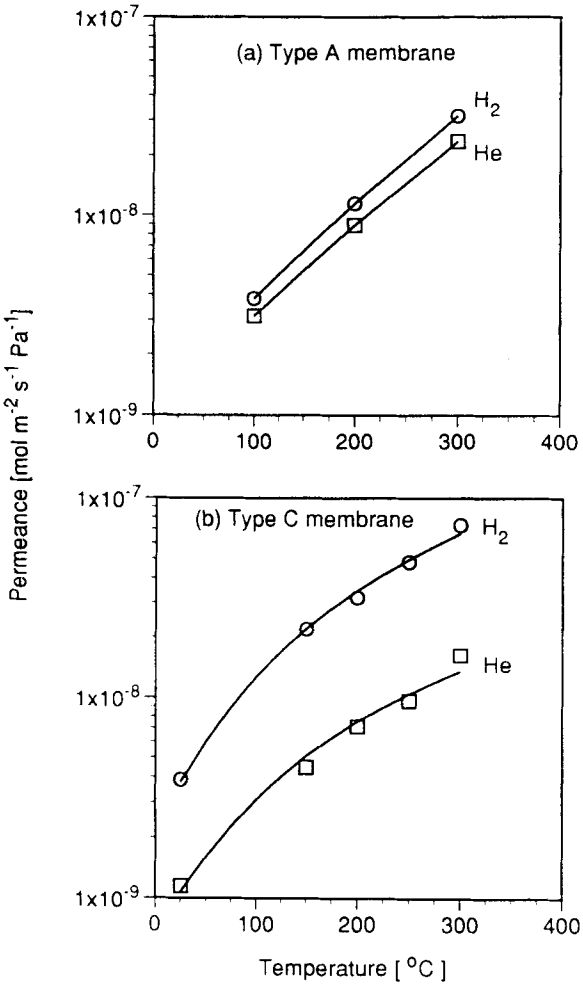

Figure 11. H_2 and He permeance vs. temperature of (a) type A and (b) type C membranes.

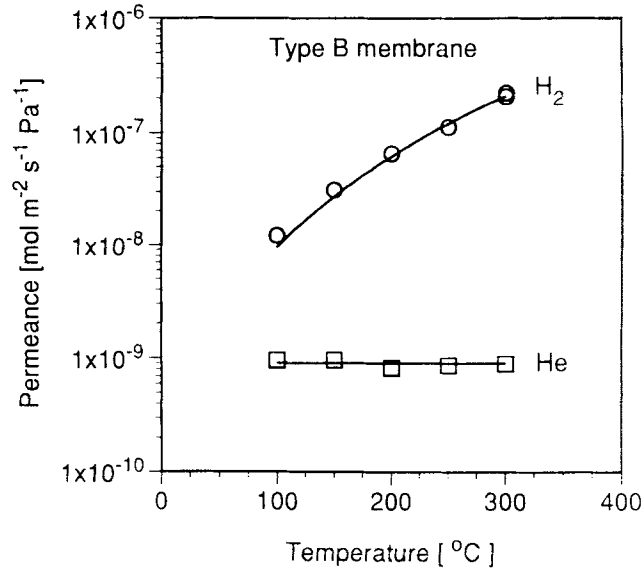

Figure 12. H_2 and He permeance vs. temperature of a type B membrane.

helium will be practically determined by R_2. Hydrogen can also permeate through the dense metal deposit (R_3). Since R_3 decreases with increasing temperature (and decreasing metal deposit thickness if bulk diffusion is rate limiting), the permeation rate of hydrogen is primarily determined by R_1. This suggests that the maximum H_2/He separation factor to be expected for the CVD-prepared Pd membranes at elevated temperatures will be of the same order of magnitude as the ratio ρ ($= R_2/R_1$). Therefore, a high value of ρ (10^2–10^3) determined at room temperature, T, after CVD is a necessary (but not sufficient) condition for achieving high selectivities for H_2 separation at elevated temperatures with the CVD-prepared Pd membranes. The preceding discussion was based on the assumption that flow of He through metal-film defects (R_2) is determined by the Knudsen mechanism at room as well as elevated temperatures, which is true if the average defect size is larger than 2 nm. Another condition is that no structural changes of the complex metallic/ceramic membranes in hand occur at elevated temperatures.

The results shown in Figures 9 and 10 indicate that the resistance through metal deposit defects (R_2) has a different dependence on temperature for Pd formed inside pores or on the surface of the γ-Al_2O_3 support. When Pd is formed inside pores of the support (type A or C membranes), R_2 shows a reversible exponential increase with temperature, while an irreversible decrease is observed when Pd covers the support surface in the form of a thin metal layer, indicating a permanent densification of type B membranes after temperature cycling. This can be explained from the different Pd growth mechanism in each situation, depicted in Figure 14. When deposition is found inside pores, precursor vapor is infiltrated inside the support, adsorbs on the surface of the γ-Al_2O_3 particles, and reacts to form Pd, which grows in the

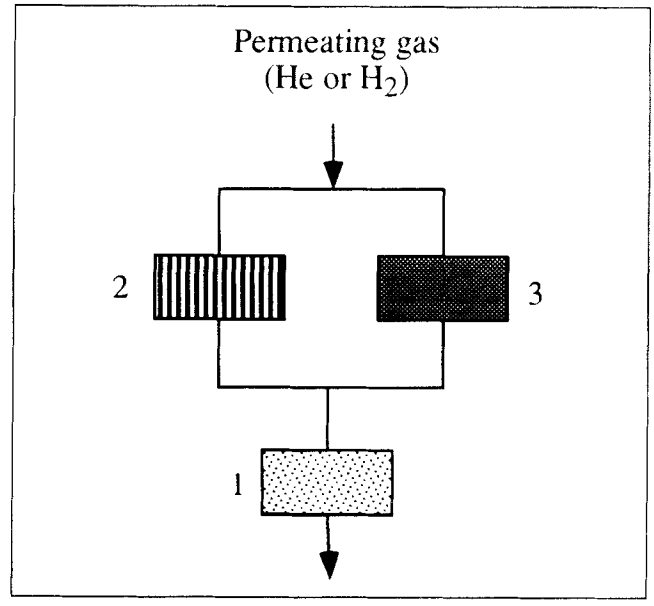

Figure 13. Resistance model for gas permeation through CVD-prepared metallic/ceramic composite membranes.

1. Porous alumina support; 2. metal film defects; 3. dense metal film.

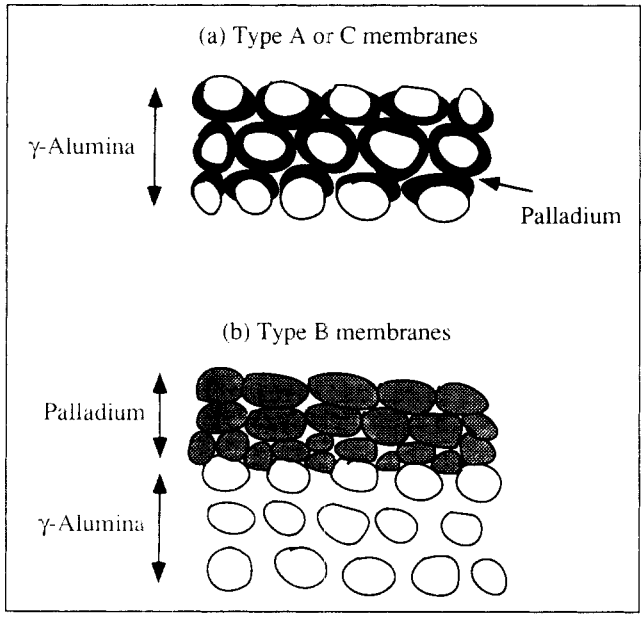

Figure 14. Different metallic/ceramic structures made by CVD: (a) inside pores or (b) on the surface of γ-Al_2O_3 supports.

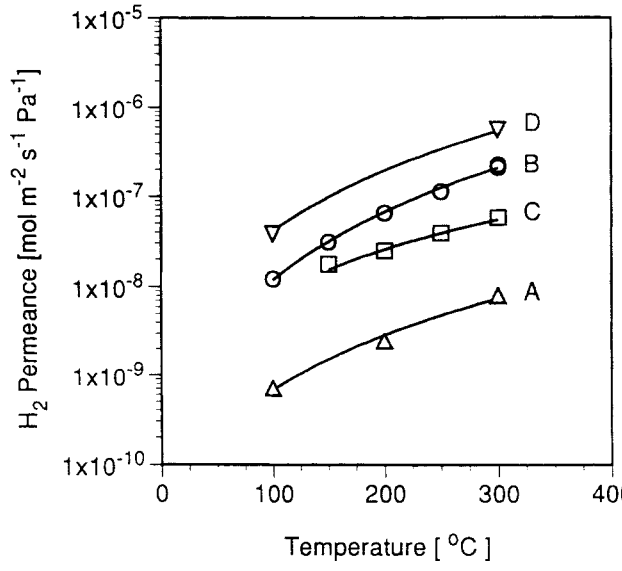

Figure 15. H_2 permeance data vs. temperature of different Pd/alumina membranes made by CVD.

(a) Type A membranes (this work); (b) type B membranes (this work); (c) type C membranes (this work); (d) Pd membrane formed in α-Al_2O_3 support by MOCVD from Pd acetate (Morooka et al., 1995).

radial direction of each particle. Pd layers from neighborhood particles when grown to a large extent form metal "bridges" resulting in the network structure shown in Figure 14a. On the other hand, when deposition is found on the support surface, nucleation of Pd begins on the external surface and grows in the outward direction only, as shown in Figure 14b.

It is obvious from the preceding picture that a much larger interaction between metal and ceramic is possible when Pd grows inside γ-Al_2O_3 pores. The observed increase of He permeance with temperature for type A or C membranes can most likely be explained by an activated diffusion mechanism through the subnanometer defects of the deposits formed inside γ-Al_2O_3 mesopores. The activation energies for He permeation through type A or C membranes were in the range 13–18 kJ/mol, similar to the values of other microporous materials reported in the literature (Kitao and Asaeda, 1991; Uhlhorn et al., 1992; Hassan et al., 1995; Bai et al., 1995). On the other hand, metal grown outside the surface of the support is independent from the ceramic, thus allowing favorable microstructural rearrangements that result in significant elimination of intercrystalline space that forms diffusion pathways for He during thermal treatment.

Figure 15 gives a comparison of H_2 permeation rates of different types of membranes prepared in/on porous alumina supports by CVD. The H_2 permeance for type A or C membranes prepared in this work was calculated by subtracting the net He permeance from that of H_2 (with H_2:He ratio < 5), and is only given here for illustration purposes. The Pd membranes made in/on macroporous supports by Morooka and coworkers (denoted as type D membranes) using Pd acetate as metal source (Yan et al., 1994; Morooka et al., 1995; Kusakabe et al., 1996) had systematically higher H_2 permeance than type B membranes prepared in this work. On the other hand, type A membranes exhibited much lower (or practically negligible) H_2 permeance, indicating that the resistance R_3 of dense material deposit (see Figure 13) is unusually high. As described earlier, type A membranes were found to consist of a mixture of poorly crystallized Pd (grain size < 5 nm) and organic material trapped inside the pores of γ-Al_2O_3, and this can explain the very low H_2 permeance of these membranes. The major difference between type B, type C, and type D membranes is the location of Pd deposition and grain size. Type B membranes formed on the surface of γ-Al_2O_3 supports in this work had an average grain size of 30–40 nm, while type D membranes formed in macropores of α-Al_2O_3 supports had grain size about 80 nm (Yan et al., 1994). Type C membranes formed in mesopores of γ-Al_2O_3 supports had average grain size about 15–20 nm, larger than that of type A membranes but smaller than those of type B or D membranes.

Figure 16 explains a possible effect of grain size on H_2 permeation through metallic membranes of different thickness. For a 100-μ-thick Pd membrane, assuming bulk atomic hydrogen diffusion rate-limiting, H_2 permeation rate will be identical to that through two 50-μm-thick Pd membranes in series, since the total membrane thickness remains the same. However, for a 1-μm-thick Pd membrane, assuming surface adsorption/desorption steps rate-limiting, H_2 permeation rate will be twice as much through two 0.5-μm-thick Pd membranes in series, since in the second case there are four surface resistances compared to two for the single membrane. If grain size determined by XRD data is a rough measure of this "fragmentation" depicted in Figure 16, it is anticipated that for thin membranes where surface steps are rate-limiting for H_2 permeation, a small grain size will result in lower apparent H_2 permeation rates at elevated temperatures. This analysis is consistent with the data in Figure 15, since the H_2 permeance of all four membrane types in-

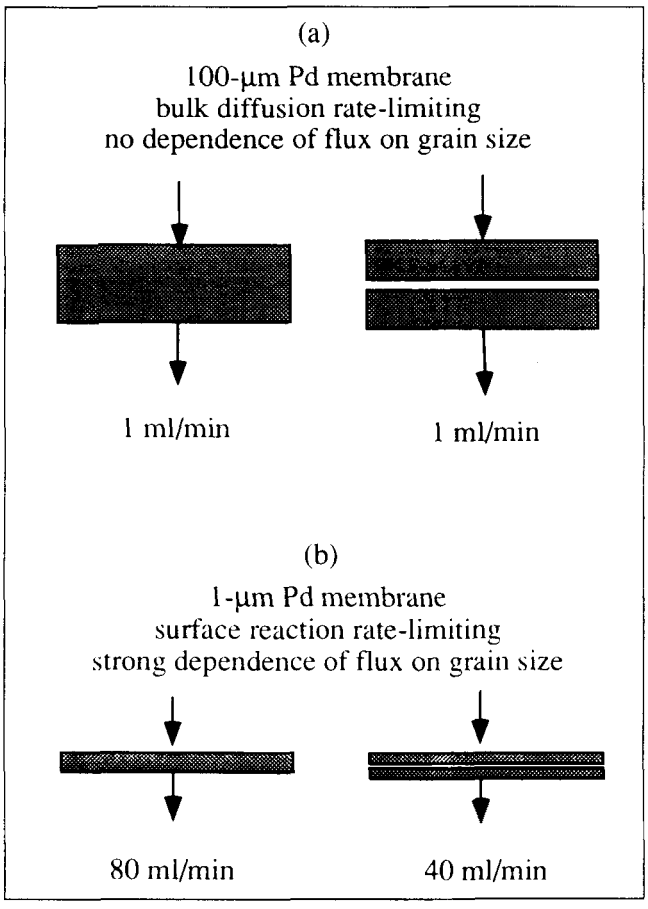

Figure 16. Effect of grain size on H_2 permeation through Pd membranes of different thickness.

creases in the same order as the average grain size of Pd formed by CVD in/on different alumina supports.

Conclusions

The gas permeation properties of thin metallic membranes prepared by CVD using different precursors and deposition conditions were studied with multicomponent permeation experiments in the temperature range 25–300°C. Pd formed inside pores or on the surface of the γ-Al_2O_3 support was effective in reducing its He permeance by about 2–4 orders of magnitude, determined at room temperature after preparation. However, the permeance of He through the metal deposit defects increased substantially with temperature when Pd was formed inside the γ-Al_2O_3 pores (type A or C membranes). On the other hand, Pd in the form of a thin film on the support surface (type B membranes) underwent favorable densification after heating to 300°C.

The permeance of H_2 was dependent on the crystallinity and morphology of the metal deposits formed by CVD. For type A membranes, H_2 permeated primarily through microporous metal deposit defects, and no permselectivity over He was observed. Type C membranes had only modest but larger than Knudsen permselectivity for H_2 over He, suggesting a parallel H_2 permeation through both microporous defects and dense metal grains. Type B membranes exhibited substantial permselectivity for H_2, while He permeance was assigned to meso/macroporous metal-film defects as implied by its weak dependence on temperature. A comparison of H_2 permeation rates of different ceramic-supported Pd membranes made by CVD suggests that the average grain size and microstructure is an important factor that determines the overall resistance for H_2 transport through these nanostructured metallic/ceramic membrane composites.

Acknowledgment

The authors are grateful for the financial support from the National Science Foundation (CTS-9216164) and to the staff of Department of Materials Science and Engineering at the University of Cincinnati for assisting in the SEM work.

Literature Cited

Bai, C., M.-D. Jia, J. L. Falconer, and R. D. Noble, "Preparation and Separation Properties of Silicalite Composite Membranes," *J. Memb. Sci.*, **105**, 79 (1995).

Bryden, K. J., and J. Y. Ying, "Nanostructured Palladium Membrane Synthesis by Magnetron Sputtering," *Mater. Sci. Eng.*, **A204**, 140 (1995).

Chang, C. H., R. Gopalan, and Y. S. Lin, "A Comparative Study on Thermal and Hydrothermal Stability of Alumina, Titania and Zirconia Membranes," *J. Memb. Sci.*, **91**, 27 (1994).

Collins, J. P., and J. D. Way, "Preparation and Characterization of a Composite Palladium-Ceramic Membrane," *Ind. Eng. Chem. Res.*, **32**, 3006 (1993).

Govind, R., and D. Atnoor, "Development of a Composite Palladium Membrane for Selective Hydrogen Separation at High Temperature," *Ind. Eng. Chem. Res.*, **30**, 591 (1991).

Hassan, M. H., J. D. Way, P. M. Thoen, and A. C. Dillon, "Single Component and Mixed Gas Transport in a Silica Hollow Fiber Membrane," *J. Memb. Sci.*, **104**, 279 (1995).

Hsieh, H. P., *Inorganic Membranes for Separation and Reaction*, Chap. 3, Elsevier, New York (1996).

Jayaraman, V., Y. S. Lin, M. Pakala, and R. Y. Lin, "Fabrication of Ultrathin Metallic Membranes on Ceramic Supports by Sputter Deposition," *J. Memb. Sci.*, **99**, 89 (1995).

Jayaraman, V., and Y. S. Lin, "Synthesis and Hydrogen Permeation Properties of Ultrathin Palladium-Silver Alloy Membranes," *J. Memb. Sci.*, **104**, 251 (1995).

Jemaa, N., J. Shu, S. Kaliaguine, and B. P. A. Grandjean, "Thin Palladium Film Formation on Shot Peening Modified Porous Stainless Steel Substrate," *Ind. Eng. Chem. Res.*, **35**, 973 (1996).

Kim, S., and G. R. Gavalas, "Preparation of H_2 Permselective Silica Membranes by Alternating Reactant Vapor Deposition," *Ind. Eng. Chem. Res.*, **103**, 211 (1995).

Kitao, S., and M. Asaeda, "Gas Separation Performance of Thin Porous Silica Membrane Prepared by Sol-Gel and CVD Methods," *Key Eng. Mater.*, **61&62**, 267 (1991).

Kusakabe, K., S. Yokoyama, S. Morooka, J.-I. Hayashi, and H. Nagata, "Development of Supported Thin Palladium Membrane and Application to Enhancement of Propane Aromatization on Ga-Silicalite Catalyst," *Chem. Eng. Sci.*, **51**, 3027 (1996).

Lin, Y. S., and A. J. Burggraaf, "Preparation and Characterization of High-Temperature Thermally Stable Alumina Membrane Composites," *J. Amer. Ceram. Soc.*, **74**, 219 (1991a).

Lin, Y. S., and A. J. Burggraaf, "Modelling and Analysis of CVD Processes in Porous Media for Ceramic Composite Preparation," *Chem. Eng. Sci.*, **46**, 3067 (1991b).

Maruyama, T., and T. Shirai, "Copper Thin Films Prepared by Chemical Vapour Deposition from Copper(II) Acetylacetonate," *J. Mater. Sci.*, **30**, 5551 (1995).

Mazanec, T. J., "Get Your O's. High Temperature Electroceramic Oxygen Separation and Reaction," *Electrochem. Soc. Interf.*, **5**, 46 (1996).

Morooka, S., S. Yan, S. Yokoyama, and K. Kusakabe, "Palladium Membrane Formed in Macropores of Support Tube by Chemical

Vapor Deposition with Crossflow Through a Porous Wall," *Sep. Sci. Technol.*, **30**, 2877 (1995).
Uemiya, S., N. Sato, H. Ando, Y. Kude, T. Matsuda, and E. Kikuchi, "Separation of Hydrogen through Palladium Thin Film Supported on a Porous Glass Tube," *J. Memb. Sci.*, **56**, 303 (1991a).
Uemiya, S., T. Matsuda, and E. Kikuchi, "Hydrogen Permeable Palladium-Silver Alloy Membrane Supported on Porous Ceramics," *J. Memb. Sci.*, **56**, 315 (1991b).
Uemiya, S., M. Koseki, and T. Kojima, "Preparation of Highly Permeable Membranes for Hydrogen Separation Using a CVD Technique," *Proc. Int. Conf. on Inorganic Membranes*, Y. H. Ma, ed., Worcester. MA, p. 545 (1994).
Uemiya, S., M. Kajiwara, and T. Kojima, "Preparation and Characterization of Composite Membranes of VIII-Group Metal Supported on Porous Alumina," *Proc. World Congress on Chemical Engineering*, San Diego, CA, p. 805 (1996).
Uhlhorn, R. J. R., K. Keizer, and A. J. Burggraaf, "Gas Transport and Separation with Ceramic Membranes. Part II. Synthesis and Separation Properties of Microporous Membranes," *J. Memb. Sci.*, **66**, 271 (1992).
Xomeritakis, G., and Y. S. Lin, "CVD of Solid Oxides in Porous Media for Ceramic Membrane Preparation or Modification. Explicit Solutions for Deposition Characteristics," *Chem. Eng. Sci.*, **23**, 3909 (1994).
Xomeritakis, G., and Y. S. Lin, "Fabrication of a Thin Palladium Membrane Supported in a Porous Ceramic Substrate by Chemical Vapor. Deposition," *J. Memb. Sci.*, **120**, 261 (1996).
Xomeritakis, G., S. Pratsinis, and Y. S. Lin, "Analysis of Ceramic Membrane Modification by CVD," *J. Chem. Vapor Depos.*, **4**, 173 (1996).
Xomeritakis, G., and Y. S. Lin, "Fabrication of Thin Metallic Membranes by MOCVD and Sputtering," *J. Memb. Sci.*, **133**, 217 (1997).
Yan, S., H. Maeda, K. Kusakabe, and S. Morooka, "Thin Palladium Membrane Formed in Support Pores by Metal-Organic Chemical Vapor Deposition and Application to Hydrogen Separation," *Ind. Eng. Chem. Res.*, **33**, 616 (1994).
Yeung, K. L., and A. Varma, "Novel Preparation Techniques for Thin Metal-Ceramic Composite Membranes," *AIChE J.*, **41**, 2131 (1995).

Manuscript received May 14, 1997, and revision received Aug. 11, 1997.